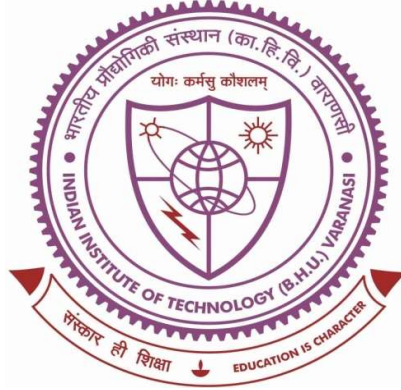


Design and Development of Extremely Low-Frequency Pulsed Electromagnetic Field Chamber for Biomedical Applications



**Thesis submitted in partial fulfillment
for the Award of Degree**

Doctor of Philosophy

by

Chandra Kant Singh Tekam

**SCHOOL OF BIOMEDICAL ENGINEERING
INDIAN INSTITUTE OF TECHNOLOGY (BHU)
(BANARAS HINDU UNIVERSITY)
VARANASI – 221005, (U.P.), INDIA**

***Dedicated
To
My Beloved Parents***

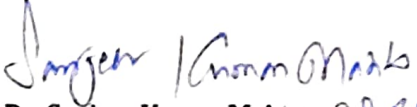
CERTIFICATE

It is certified that the work contained in the thesis titled "Design and Development of Extremely Low-Frequency Pulsed Electromagnetic Field Chamber for Biomedical Applications" by "Chandra Kant Singh Tekam" has been carried out under my supervision and that this work has not been submitted elsewhere for a degree.

It is further certified that the student has fulfilled all the requirements of Comprehensive, Candidacy and SOTA for the award of Ph.D. degree.

Date: 28/06/2023

Place: Varanasi


Dr. Sanjeev Kumar Mahto 28.06.23
(Supervisor)

SUPERVISOR

DECLARATION BY THE CANDIDATE

I, **Chandra Kant Singh Tekam**, certify that the work embodied in this Ph.D. thesis is my own bonafide work carried out by me under the supervision of **Dr. Sanjeev Kumar Mahto** for a period from **July 2016** to **June 2023** at the **SCHOOL OF BIOMEDICAL ENGINEERING**, Indian Institute of Technology (Banaras Hindu University), Varanasi, India. The matter embodied in this Ph.D. thesis has not been submitted for the award of any other degree/diploma. I declare that I have faithfully acknowledged and given credits to the research workers wherever their works have been cited in my work in this thesis. I further declare that I have not willfully copied any other's work, paragraphs, text, data, results, *etc.*, reported in journals, books, magazines, reports dissertations, thesis, *etc.*, or available at websites and have not included them in this thesis and have not cited as my own work.

Date...28/06/2023

Place: Varanasi


(Chandra Kant Singh Tekam)

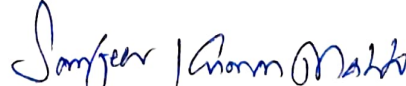
CERTIFICATE BY THE SUPERVISOR

This is to certify that the above statement made by the candidate is correct to the best of my knowledge.


Dr. Sanjeev Kumar Mahto 28.06.23

Supervisor

SUPERVISOR


Dr. Sanjeev Kumar Mahto 28.06.23

Coordinator

समन्वयक/CO-ORDINATOR

जैव चिकित्सा अभियांत्रिकी स्कूल
SCHOOL OF BIOMEDICAL ENGG
भारतीय प्रौद्योगिकी संस्थान (का.हि.वि.)
INDIAN INSTITUTE OF TECHNOLOGY (B.H.U.)
वाराणसी 221005/VARANASI-221005

COPYRIGHT TRANSFER CERTIFICATE

Title of the Thesis: Design and Development of Extremely Low-Frequency Pulsed
Electromagnetic Field Chamber for Biomedical Applications.

Name of Student: Chandra Kant Singh Tekam

Copyright Transfer

The undersigned hereby assigns to the Indian Institute of Technology (Banaras Hindu University), Varanasi all rights under copyright that may exist in and for the above thesis submitted for the award of the Doctor of Philosophy.

Date: 28/06/2023

Place: Varanasi



(Chandra Kant Singh Tekam)

Note: However, the author may reproduce or authorize others to reproduce material extracted verbatim from the thesis or derivative of the thesis for author's personal use provided that the source and the Institute's copyright notice are indicated.

ACKNOWLEDGEMENTS

It is my greatest pleasure to have this opportunity to express my sincere appreciation to everyone who helped me during my Ph.D. program at the Indian Institute of Technology (Banaras Hindu University), Varanasi. First, I want to thank my supervisor, Dr. Sanjeev Kumar Mahto, for his valuable guidance, encouragement, and paternal behavior throughout the work. His inspiring and excellent guidance is the key reason I could successfully finish each research objective. This work would not have been possible without his guidance as a great mentor.

I want to thank my research progress evaluation committee (RPEC) members, Prof. Sairam Krishnamurthy and Dr. Deepesh Kumar, for cooperating during this work. I offer my special thanks to **Dr. Sanjeev Kumar Mahto**, Coordinator of the School of Biomedical Engineering, for providing all the necessary facilities of the school. I want to express my sincere gratitude to Prof. Ranjana Patnaik for her valuable input, suggestions, and affectionate mannerism.

I wish to express deep regards to all the teachers of the Department, Prof. Neeraj Sharma, Dr. Sanjay Kumar Rai, Dr. Shiru Sharma, Dr. Pradeep Paik, and others, for their kind support during my research.

I want to thank Prof. Vikash Kumar Dubey, In-Charge, Central Instrument Facility Centre and his team members for providing all the characterization facilities on time with precision, without which the completion of this work was impossible. I also wish to thank all other respected faculty members of the school for their kind support and valuable suggestions.

A special thanks to my teammates Dr. Ajay Kumar Sahi, Ms. Pooja Kumari, Ms. Shrivanya Gundu, Ms. Shreyasi Majumdar, and Dr. Santosh Kumar Prajapati for their suggestions and healthy discussion of my research issues. I would also like to thank my lab mates

Neelima, Snehalata, Parul, Richa, and Sushmitha for their support and encouragement. I am extremely thankful to my friends and seniors, Mr. Pankaj Kumar Jain, Mr. Neeraj Sharma, and Dr. Gaurav Kumar, for their support, cooperation, and sincere help in many ways as well as for making my stay here enjoyable and for their time-to-time encouragement during my bad situations.

I sincerely thank all the school's supporting staff for their kind help whenever I required it.

I can never forget my parents, Mr. Manohar Singh Tekam & Mrs. Devki Singh Tekam; my brother Dr. Chandra Shekhar Singh Tekam; my Bhabhi Mamta Paraste; my nephew Ayansh and my niece Moon whose boundless love, constant inspiration, emotional support and blessings has encouraged me at every step of life. My parents' everlasting shower of blessing kept me moving easily, with all hazards vanishing miraculously. My word power fails to express my gratitude to my loving family members for their encouragement and moral support during my work.

Lastly, I would like to thank Almighty for making everything possible by giving me the strength and courage to do this work.

(Chandra Kant Singh Tekam)

Date:

Place: Varanasi

LIST OF FIGURES

Figure No.	Figure description	Page No.
Figure 1.1	Schematic representation of EFs. (A) EF from an isolated negative charge, (B) EF from an isolated positive charge, (C) EFs lines from the opposite charges.	06
Figure 1.2	Schematic representation of MFs from different sources. (A) Bar magnet, (B) Current carrying wire, (C) Horseshoe magnet.	07
Figure 1.3	Schematic representation of magnetic force. (A) Magnetic force on moving charge, (B) Magnetic force on straight wire of length L.	09
Figure 1.4	Schematic representation of magnetic flux through flat surface.	10
Figure 1.5	Schematic representation of geomagnetic field of Earth.	11
Figure 1.6	50 Hz ELF-PEMF exposure for treatment of various diseases, including cancer and skeletal muscle disorders.	25
Figure 1.7	State of the art of magnetic field exposure.	26
Figure 2.1	Biot-Savart law. (A) Magnetic field generation at point "P" along section (dl) at radial distance (r), (B) The representation of the magnetic field orientation along wire length.	48
Figure 2.2	Structural configuration of Helmholtz coil system. (A) Schematic of Helmholtz coils, (B) MF orientation due to current flow inside coils. All dimensions are given in meters.	51
Figure 2.3	Relationship between wire gauge, coil current, and wire resistance. (A) Relationship between wire resistance and wire gauge, (B) Relationship between coil current and wire gauge.	52
Figure 2.4	Spatial limitations in the development of Helmholtz coils. (A) Relationship between coil current and wire gauge when no. of wire turns (N) is 300 turns/coil, (B) Relationship between coil current and wire gauge when no. of wire turns (N) is 540 turns/coil, (C) Relationship between coil current and wire gauge when no. of wire turns (N) is 1000 turns/coil, (D) Relationship between coil current and wire gauge when no. of wire turns (N) is 2000 turns/coil.	54
Figure 2.5	Relationship between magnetic flux density, wire radius, cross-sectional area and wire gauge. (A) Relationship between magnetic flux density and wire gauge, (B) Relationship between wire radius and wire gauge, (C) Relationship between cross-sectional area and	55

	wire gauge, (D) Relationship between coil current and wire resistance.	
Figure 2.6	Magnetic flux density and MF intensity between Helmholtz coils at different current intensities. (A) Magnetic flux density and MF intensity at y-axis (I = 1 A), (B) Magnetic flux density and MF intensity at y-axis (I = 2 A), (C) Magnetic flux density and MF intensity at y-axis (I = 3 A).	62
Figure 2.7	MF overlay between Helmholtz coils at different current intensities. (A) MF overlay at yz-plane (I = 1 A), (B) MF overlay at yz-plane (I = 2 A), (C) MF overlay at yz-plane (I = 3 A).	63
Figure 2.8	Mono-axial Helmholtz coil (parallel configuration) for bioelectromagnetic studies. (A) Schematic representation for 50 Hz ELF-PEMF chambers, (B) Custom-made 50 Hz ELF-PEMF chamber for <i>in vivo</i> and <i>in vitro</i> studies.	65
Figure 2.9	Schematic of experimental MF measurement with acrylic sheet arrangement with equidistant holes.	67
Figure 2.10	50 Hz ELF-PEMF distributions between Helmholtz coils at different loading voltages. (A) Magnetic flux density vs. sensor movement along the z-axis for a voltage and current range (V = 75 volts, I = 1.0 A), (B) Magnetic flux density vs. sensor movement along the z-axis for a voltage and current range (V = 132 volts, I = 2.0 A), (C) Magnetic flux density vs. sensor movement along the z-axis for a voltage and current range (V = 189 volts, I = 3.0 A).	68
Figure 3.1	Schematic representation of Helmholtz coil system. (A) Monoaxial Helmholtz coil structural profile, (B) magnetic field direction inside exposure system, (C) Sinusoidal current characteristics, (D) Schematic arrangement of the Helmholtz coil setup for bioelectromagnetic studies.	80
Figure 3.2	50 Hz ELF-PEMF exposure system for <i>in vitro</i> and <i>in vivo</i> experiments. (A) Schematic representation for <i>in vivo</i> analysis, (B) Schematic representation for <i>in vitro</i> study, (C) Monoaxial Helmholtz coil system for <i>in vivo</i> analysis, (D) Monoaxial Helmholtz coil system for <i>in vitro</i> analysis.	81
Figure 3.3	50 Hz ELF-PEMF distributions between Helmholtz coils at different loading voltages. (A) Schematic for acrylic sheet placement along x, y, and z-axis in 50 Hz ELF-PEMF exposure system (B) Magnetic flux density vs sensor movement along the z-	82

	axis for a voltage and current range ($V = 75$ volts, $I = 1.0$ A), (C) Magnetic flux density vs sensor movement along the z-axis for a voltage and current range ($V = 120$ volts, $I = 2.0$ A), (D) Magnetic flux density vs sensor movement along the z-axis for a voltage and current range ($V = 190$ volts, $I = 3.0$ A).	
Figure 3.4	Schematic representation of repeated 5-day MF exposure study. In this study, C6 cell lines were exposed to 50 Hz ELF-PEMF (1-3 mT, 20 min (twice) with 4 h gap) under <i>in vitro</i> conditions and observed daily for changes in cell proliferation and morphology.	83
Figure 3.5	Schematic representation of repeated 14 days <i>in vivo</i> study. In this study, adult Wistar rats were exposed to 50 Hz ELF-PEMF exposure (1-3 mT, 20 min (twice) with a 4 h gap). We observed any significant changes in total body weight, organ coefficient, cognitive abilities, brain tissue structure, and morphology.	87
Figure 3.6	Schematic representation of Y-maze test for spontaneous	89
Figure 3.7	Influence of 50 Hz ELF-PEMF on the proliferation and morphology of C6 cell lines. (A) A representative panel of bright-field images of C6 cells stimulated by ELF-PEMF of different strengths, (B) a Representative panel of fluorescent images of C6 cells stimulated by ELF-PEMF of varying strength, (C) C6 cells count at different MF intensities over 5 days. The initial seeding concentration was 1×10^3 cells/well and ELF-PEMF with an exposure duration of 20 min (twice) with a 4 h gap till the 6 th day or confluency (90%). Scale bar: 100 μ m for bright-field, fluorescent, and merged images. The values are expressed as mean \pm S.D.	92
Figure 3.8	50 Hz ELF-PEMF influence on organ coefficient of the brain and total body weight. (A) Organ coefficient of brain, (B) Total body weight. The values are expressed as mean \pm S.D. ($n = 6$).	93
Figure 3.9	Influence of 50 Hz ELF-PEMF on spontaneous alternation, anxiety, motor coordination, and locomotor activity of adult Wistar rats. (A) Total arm entries Trial-1, (B) Total arm entries Trial-2, (C) Percentage known arm entries, (D) Percentage known novel arm entries, (E) Percentage open arm entries, (F) Percentage time spent in open arms, (G) Total arm entries, (H) Retention time on rod (sec.), (I) Locomotor activity (score/5 min.). Two-way ANOVA was utilized for statistical analysis, and values are expressed as mean \pm S.D. ($n = 6$).	99
Figure 3.10	Influence of 50 Hz ELF-PEMF exposure on hippocampus and cortex brain region. Representative H&E-stained images of brain tissues in control and ELF-PEMF exposed groups on day 14; (A)	100

	Hippocampus DG region (control, 1 mT, 2 mT & 3 mT), (B) Hippocampus CA2 region (control, 1 mT, 2 mT & 3 mT), (C) cortex region (control, 1 mT, 2 mT & 3 mT), (D) cortex cell count in exposed and control groups. No aberrant changes existed between control, ELF-PEMF1, ELF-PEMF2, and ELF-PEMF3 exposed rats. The values are expressed as mean \pm S.D. (n = 6).	
Figure 4.1	50 Hz ELF-PEMF exposure system. (A) Schematic of horizontal magnetic field generating system, (B) Schematic for placement of exposure space (black arrow and red arrow indicate the magnetic field direction and current direction inside coils respectively), (C) Schematic representation of exposure system (<i>in vivo</i> model), (D) Schematic representation of PEMF exposure (<i>in vitro</i> model), (E) Prototype of horizontal magnetic field exposure system (<i>in vivo</i> model), (F) Prototype of horizontal magnetic field exposure system (<i>in vitro</i> model).	121
Figure 4.2	Schematic representation of repeated 5-day <i>in vitro</i> study. In this study, we exposed the cell culture to PEMF exposure (1-3 mT, 20 min (twice) with a 4 h gap) and observed any sign of a reduction in the proliferative activity of cells.	124
Figure 4.3	Schematic representation of repeated 14 days <i>in vivo</i> study. In this study, adult Wistar rats were exposed to 50 Hz ELF-PEMF exposure (1-3 mT, 20 min (twice) with a 4 h gap) and were observed for any sign of toxicity.	126
Figure 4.4	Effect of 50 Hz magnetic field (1-3 mT, 20 min (twice) with 4 h gap) on the proliferation and morphology of the RFP-L929 fibroblast cells. (A) Representative panel of brightfield images of RFP-L929 cells stimulated by the magnetic field compared to control, (B) RFP-L929 cell count at different magnetic field intensities over 5 days compared to control, (C) Representative panel for fluorescent images of RFP-L929 exposed to magnetic field intensities compared to control. The initial seeding concentration was 1×10^3 cells/well and magnetic field with an exposure till the 5th day or confluency (90%). Scale bar: 100 μ m for brightfield and fluorescent images. The values are expressed as mean \pm S.D. (n = 6), and the level of significance is * $p < 0.05$, ** $p < 0.01$, *** $p < 0.001$.	130
Figure 4.5	Effect of magnetic field (1-3 mT, 20 min (twice) with 4 h gap) on organ coefficient and total body mass. (A) Organ coefficient of the liver, (B) Organ coefficient of the kidney, (C) Organ coefficient of the heart, (D) Total body mass of rats. One-way ANOVA found	132

	significant differences. The values are expressed as mean \pm S.D. (n = 6), and $p < 0.05$ is considered statistically significant.	
Figure 4.6	Effect of 50 Hz ELF-PEMF (1-3 mT, 20 min (twice) with 4 h gap) on blood serum concentration of (A) AST, (B) ALT, (C) Total bilirubin, (D) Ck-MB, (E) serum creatinine at the end of the experimental period. The values are expressed as mean \pm S.D. (n = 6 male rats/groups), and the level of significance is * $p < 0.05$, ** $p < 0.01$, *** $p < 0.001$. (One-way ANOVA followed by Tukey's multiple comparison post hoc test).	135
Figure 4.7	Effect of 50 Hz ELF-PEMF (1-3 mT, 20 min (twice) with 4 h gap) on organs like liver, kidney, and heart tissue stained with hematoxylin and eosin.	137
Figure 5.1	50 Hz ELF-PEMF exposure system. (A) Schema of horizontal MF generating system, (B) Schema for MF exposure (blue arrows indicate the MF direction), (C) A.C. current characteristics, (D) Schema for MF exposure chamber for <i>in vitro</i> analysis (temperature and humidity controlled), (E) Arrangement of power supply and digital display monitoring system, (F) Prototype of horizontal MF exposure system. Right photograph shows a 2-D alternating MF generating monoaxial coil system. Inner cubic box is an incubation chamber for cell cultivation. Left photograph shows combination of A.C. power supplies, autotransformer and digital ammeter/voltmeter for continuous monitoring.	160
Figure 5.2	Schematic representation experimental protocol for repeated 5-days magnetic field exposure study. In this study, different cancer cell lines were exposed to 50 Hz magnetic field (1-3 mT, 20 min (twice) with 4 h gap) under <i>in vitro</i> conditions and observed daily for effect on cell proliferation.	163
Figure 5.3	Mechanism of MTT assay to determine the cellular proliferation.	165
Figure 5.4	Cell count % of adenocarcinoma (A549) cells was significantly affected by the 50 Hz ELF-PEMF exposure (horizontally aligned). A549 cells were counted at different MF intensities (1-3 mT, 20 min (twice) with a 4 h gap) over 5 days. (A) Effects of 1 mT on A549 cell count compared to control, (B) Effects of 2 mT on A549 cell count compared to control, (C) Effects of 3 mT on A549 cell count compared to control, (D) Comparative analysis of MF exposure on A549 cells compared to the control group. The initial seeding concentration was 1×10^3 cells/well, and magnetic field exposure till the 5th day or confluency ($\geq 95\%$). The independent exposures	167

	were performed in triplicates. “*” $p < 0.05$, “**” $p < 0.01$, “***” $p < 0.001$.	
Figure 5.5	Cell count % of breast cancer (MCF-7) cells was found unaffected by the to 50 Hz ELF-PEMF (horizontally aligned) exposure. MCF-7 cells count at different MF intensities (1-3 mT, 20 min (twice) with 4 h gap) over 5 days. (A) Effects of 1 mT on MCF-7 cell count compared to control, (B) Effects of 2 mT on MCF-7 cell count compared to control, (C) Effects of 3 mT on MCF-7 cell count compared to control, (D) Comparative analysis of MF exposure on MCF-7 cells compared to control group. The initial seeding concentration was 1×10^3 cells/well, and MF exposure till the 5 th day or confluency ($\geq 95\%$). The independent exposures were performed in triplicates. “*” $p < 0.05$, “**” $p < 0.01$, “***” $p < 0.001$.	168
Figure 5.6	Cell count% of hepatoblastoma (HepG2) cells was unaffected by the 50 Hz ELF-PEMF exposure (horizontally aligned). HepG2 cells count at different MF intensities (1-3 mT, 20 min (twice) with 4 h gap) over 5 days. (A) Effects of 1 mT on HepG2 cell count compared to control, (B) Effects of 2 mT on HepG2 cell count compared to control, (C) Effects of 3 mT on HepG2 cell count compared to control, (D) Comparative analysis of MF exposure on HepG2 cells compared to control group. The initial seeding concentration was 1×10^3 cells/well, and MF exposure till the 5 th day or confluency ($\geq 95\%$). The independent exposures were performed in triplicates. “*” $p < 0.05$, “**” $p < 0.01$, “***” $p < 0.001$.	169
Figure 5.7	Effects of 50 Hz ELF-PEMF exposure (1-3 mT, 20 min (twice) with 4 h gap) on cell proliferation and morphology of A549 cells as observed through the analysis of microscopic images. (A) A representative panel of bright-field images of A549 cells stimulated by magnetic field of different strengths, (B) A representative panel of fluorescent images of A549 cells stimulated by magnetic field of different strengths. Scale bar: 100 μm for bright-field, fluorescent, and merged images.	170
Figure 5.8	Effect 50 Hz ELF-PEMF exposure (1-3 mT, 20 min (twice) with 4 h gap) on proliferation and morphology of MCF-7 and HepG2 cells as observed through qualitative analysis of microscopic images. (A) A representative panel of bright-field images of MCF-7 cells stimulated by magnetic field of different strengths, (B) A representative panel of fluorescent images of HepG2 cells stimulated by magnetic field of different strengths. Scale bar: 100 μm for bright-field images.	171

Figure 5.9	Effects of 50 Hz ELF-PEMF exposure (1-3 mT) on cell viabilities of A549 cells compared with control. Cells were incubated for 5 days or confluency ($\geq 95\%$), and magnetic field was applied daily for the indicated duration. (A) A549 cells exposed with 1 mT compared with control, (B) A549 cells exposed with 2 mT compared with control, (C) A549 cells exposed with 3 mT compared with control, (D) Comparative analysis of magnetic field exposure on A549 cells. The independent exposures were performed in triplicates. “*” $p < 0.05$, “**” $p < 0.01$, “***” $p < 0.001$.	173
Figure 5.10	Effects of 50 Hz ELF-PEMF exposure (1-3 mT) on cell viabilities of MCF-7 cells compared with control. Cells were incubated for 5 days or confluency ($\geq 95\%$), and magnetic field was applied daily for the indicated duration. (A) MCF-7 cells exposed with 1 mT compared with control, (B) MCF-7 cells exposed with 2 mT compared with control, (C) MCF-7 cells exposed with 3 mT compared with control, (D) Comparative analysis of magnetic field exposure on MCF-7 cells. The independent exposures were performed in triplicates. “*” $p < 0.05$, “**” $p < 0.01$, “***” $p < 0.001$.	174
Figure 5.11	Effects of 50 Hz ELF-PEMF exposure (1-3 mT) on cell viabilities of HepG2 cells compared with control. Cells were incubated for 5 days or confluency ($\geq 95\%$), and magnetic field was applied daily for the indicated duration. (A) HepG2 cells exposed with 1 mT compared with control, (B) HepG2 cells exposed with 2 mT compared with control, (C) HepG2 cells exposed with 3 mT compared with control, (D) Comparative analysis of magnetic field exposure on HepG2 cells. The independent exposures were performed in triplicates. “*” $p < 0.05$, “**” $p < 0.01$, “***” $p < 0.001$.	175

LIST OF TABLES

Table No.	Table description	Page No.
Table 1.1	Typical magnetic field levels near household appliances.	12
Table 1.2	Typical MF levels near power lines.	13
Table 1.3	The experimental studies to assess the effectiveness of 50 Hz ELF-PEMF exposure as an alternative diagnostic or therapeutic method.	21
Table 2.1	Theoretical electrical parameters for Helmholtz coil system.	59
Table 2.2	Electrical parameters obtained on Helmholtz coil prototype.	59
Table 2.3	Electrical parameters obtained for generation and maintenance of uniform magnetic field.	60
Table 2.4	Magnetic field homogeneity at the center of the Helmholtz coil system for $I = 1 - 3$ A.	69
Table 2.5	Temperature variation in coils during the experimental duration.	69
Table 3.1	Effect of 50 Hz ELF-PEMF exposure (1-3 mT) on organ coefficient of the brain of rats.	93
Table 3.2	Effect of 50 Hz ELF-PEMF exposure (1-3 mT) on total body weight of rats.	94
Table 3.3	Effects of 50 Hz ELF-PEMF exposure (1-3 mT) on behavioral changes in adult Wistar rats during Y-maze, EPM, Rotarod, and Actophotometer test.	96
Table 4.1	Design specification of 50 Hz ELF-PEMF exposure system.	120
Table 4.2	Effect of 50 Hz ELF-PEMF exposure (1-3 mT, 20 min (twice) with 4 h gap) on organ coefficients (liver, heart, and kidney) of adult Wistar rats.	132
Table 4.3	Effect of 50 Hz ELF-PEMF exposure (1-3 mT, 20 min (twice) with 4 h gap) on total body mass of adult Wistar rats.	133
Table 4.4	Effect of 50 Hz ELF-PEMF exposure (1-3 mT, 20 min (twice) with 4 h gap) on serum enzymes of adult Wistar rats.	136
Table 4.5	Summary of 50 Hz ELF-PEMF exposure (1-3 mT) effects on biochemical parameters, organ coefficient, and total body mass of rats.	138
Table 5.1	Design specification of 50 Hz ELF-PEMF exposure system.	158

Table 5.2	Effect of 50 Hz ELF-PEMF exposure (1-3 mT) on A549 cells assessed through the MTT assay.	172
Table 5.3	Effect of 50 ELF-PEMF exposure (1-3 mT) on MCF-7 cells assessed through the MTT assay.	172
Table 5.4	Effect 50 Hz ELF-PEMF exposure (1-3 mT) on HepG2 cells assessed through the MTT assay	173
Table 5.5	Effects of 50 Hz magnetic field exposure on cell morphology of different cancer cell lines.	175

LIST OF ABBREVIATIONS AND SYMBOLS

EM	Electromagnetic
ELF	Extremely low-frequency
ELF-PEMF	Extremely low frequency pulsed electromagnetic field
Hz	Hertz
kHz	Kilohertz
GHz	Gigahertz
AC	Alternating current
DC	Direct current
λ	Wavelength
c	Speed of light in vacuum
E	Energy
h	Plank's constant
ν	Frequency
VLF	Very low frequency
RF	Radiofrequency
MF	Magnetic field
EF	Electric field
E	Electric field strength
B	Magnetic flux density
T	Tesla
μ_0	Permeability of free space
μ_r	Permeability of magnetic material
d l	Vector line segment
I	Current flow in conductor
G	Gauss
mG	Milligauss
kV	Kilovolt
H	Magnetic field strength
F _c	Faraday's constant
A	Crosssectional area
F	Force
q	Charge

μT	Microtesla
nT	Nanotesla
χ	Magnetic susceptibility
M	Magnetization
ODC	Ornithine decarboxylase
TBIL	Total bilirubin
WBC	White blood cell
SMF	Static magnetic field
ND	Neurodegenerative
PHB	Primary human brain
REMF	Repeated electromagnetic field stimulation
BAP	Amyloid- β protein
PC	Protein carbonyl
MDA	Malondialdehyde
PEF	Pulsed electric field
nsPEF	Nanosecond pulsed electric field
TRIMprob	Tissue resonance interaction method
LEET	Low energy emission therapy
TTF	Tumour treatment fields
SD	Sprague-Dawley
BSA	Bovine serum albumin
DAPI	4',6-diamidino-2-phenylindole
CAEC	Central animal ethical committee
ANOVA	Analysis of variance
PAS	Periodic acid-schiff
CNS	Central nervous system
PNS	Peripheral nervous system
ICNIRP	International commission on non-ionizing radiation protection
MRI	Magnetic resonance imaging
miRNA	Micro ribonucleic acid
DNA	Deoxyribonucleic acid
$\frac{dB}{dt}$	Rate of change of magnetic field

A549	Lung adenocarcinoma cell line
GIST-T1	Human gastrointestinal stromal cancer cell line
HCT116	Human colon cancer cell line
PC9	Human lung cancer cell line
LFRSMF	Low frequency rotating static magnetic field
MCF7	Breast cancer cell line
MCF10	Non-tumorigenic cell line
NIH3T3	Fibroblast cell line
HL60	Human leukemia cell line
K562	Lymphoblast cell line
A375	Human malignant melanoma cell line
H4	Human neuroglioma cell line
SaOS-2	Human osteosarcoma cell line
HepG2	Hepatocellular carcinoma cell line
ALP	Alkaline phosphate
MNPs	Magnetic nanoparticles
ROS	Reactive oxygen species
MDA-MB231	Breast cancer cell line
SW480	Colon cancer cell line
HL7702	Normal human liver cells
Bel7402	Human liver carcinoma cell line
U251	Glioblastoma cancer cell line
AFP	Alpha fetoprotein
UP-TTD	Ultrasound powered device
AST	Aspartate aminotransferases
ALT	Alanine aminotransferases
CK-MB	Creatine phosphokinase mb
MTT	3-(4,5-dimethylthiazol-2-yl)-2,5-diphenyltetrazolium bromide
R_c	Radius of coil
N	Number of wires turns
D	Coil separation distance
d_w	Wire diameter

R	Resistance of wire
ρ	Resistivity of wire
SWG	Standard wire gauge
PTSD	Post traumatic stress disorder
ATP	Adenosine triphosphate
C6	Glial cell line
NCCS	National centre for cell sciences
DMEM	Dulbecco's modified eagle's medium
PBS	Phosphate buffer saline
FBS	Fetal bovine serum
EDTA	Ethylenediaminetetraacetic acid
EPM	Elevated plus maze
DG	Dentate gyrus
CA	Cornu ammonis
SD	Standard deviation
APP	Amyloid precursor protein
TMZ	Temozolomide
GBM	Glioblastoma multiforme cell line
IAEC	Institute animal ethical committee
RBC	Red blood cells
RFP-L929	Red fluorescent protein mouse fibroblast cell line
H&E	Haematoxylin and eosin
ULF-PEMF	Ultralow frequency pulsed electromagnetic field
PC12	Pheochromocytoma
F-actin	Filamentous actin
293T	Human embryonic kidney cell line

Extremely low-frequency pulsed electromagnetic fields (ELF-PEMF) are omnipresent in our environment due to the rise in industrial activity, transmission lines, and household applications of electrical and electronic devices. A wider range of electrical and electronic device-generated magnetic fields are considered safe. Numerous studies have been done to look into the potential health impacts of long-term ELF-PEMF exposure (≥ 1 h/day). However, the scientific evidence is mixed, and more research is needed to establish conclusive findings for exposure duration (≤ 1 h/day). The biological effects of magnetic fields primarily depend on magnetic flux density, frequency, and duration. Moreover, biological effects can be divided into thermal and non-thermal, which cause membrane depolarization, excitation, and electrostimulation. The World health organization (WHO) also considers the rising electromagnetic fields in the environment a potential health concern worldwide. However, some studies have also reported the applications of extremely low frequency (ELF) fields for treating neurological, muscle, and cancer disorders. ELF-PEMF is a non-invasive, cost-effective therapeutic technique that uses low-intensity, low frequency magnetic fields for treatment of various diseases.

We have designed, fabricated, characterized, and applied uniform magnetic flux densities for bioelectromagnetic studies under *in vivo* and *in vitro* conditions. The computational simulation was performed on ANSYS electromagnetic suite (18.0) to determine the magnetic flux densities and behaviors of magnetic flux lines. The effects of ELF-PEMF on cell lines (C6, RFP-L929, A549, MCF-7, and HepG2) as well as on behavioral (spontaneous alternation, anxiety, motor coordination, and locomotor activity) and biochemical parameters (AST, ALT, bilirubin, serum creatinine, and CK-MB) of rats were studied under *in vitro* and *in vivo* conditions, respectively, using the custom-made

monoaxial Helmholtz coil. The ELF-PEMF effects on various behavioral, biochemical, and histological parameters were performed to determine the onset of harmful effects at early stages; however, no harmful effects were incidentally observed under the present experimental conditions. Additionally, we have devised a novel therapeutic approach to kill cancer cells. Results have also shown that the magnetic field noticeably induced cell death in lung adenocarcinoma (A549) cells under *in vitro* conditions.

The magnetic field may provide a novel non-invasive approach to cancer treatment and thus offers advantages over other methods to increase patient safety. The magnetic field treatment can also be supplemented by metal nanoparticles for drug delivery, magnetically modified scaffold for wound healing, and peripheral nerve injury. Further studies must determine the exact molecular mechanism for such therapeutic purposes.

Keywords:

ELF-PEMF, Spontaneous alternation, Anxiety, A549, MCF7, C6, RFP-L929, AST, ALT, Ck-MB.